



## Paper based field deployable sensor for naked eye monitoring of copper (II) ions; elucidation of binding mechanism by DFT studies

Halali V. Vishaka<sup>a</sup>, Manav Saxena<sup>a</sup>, H.R. Chandan<sup>a</sup>, Anupam Anand Ojha<sup>b</sup>, R. Geetha Balakrishna<sup>a,\*</sup>

<sup>a</sup> Centre for Nano and Material Sciences, Jain University, Ramanagaram, Bangalore 562112, India

<sup>b</sup> Laboratory of Physical Chemistry, ETH Zurich, Switzerland

### ARTICLE INFO

#### Article history:

Received 11 March 2019

Received in revised form 17 June 2019

Accepted 17 June 2019

Available online 19 June 2019

#### Keywords:

Colorimetric probe  
Selective and sensitive  
Cu<sup>2+</sup> detection  
Blood samples  
DFT

### ABSTRACT

The study demonstrates the fabrication of test strips made from newly synthesized ortho-Vanillin based colorimetric chemosensor (probe **P**) that could be employed as field deployable tool for rapid and naked eye detection of Cu<sup>2+</sup>. Upon addition of Cu<sup>2+</sup> to the chemosensor, it exhibits rapid pink color from colorless and can be easily seen through the naked eye. This probe exhibits a remarkable colorimetric “ON” response and the absorbance intensity of the probe enhances significantly in presence of Cu<sup>2+</sup>. The sensing mechanism has been deduced using FTIR, XPS, LCMS and DFT studies. The binding mechanism of the probe to Cu<sup>2+</sup> was substantiated by DFT studies. HOMO of the probe suggests that a high electronic density resides on O, N atoms and thus these are the favorable binding site for the metal ions. Study revealed that the **P** + Cu<sup>2+</sup> complex is  $-35.64$  eV more stable than individual reactants. The Cu<sup>2+</sup> binds to the probe in 1:1 stoichiometry with a binding constant of  $2.6 \times 10^4 \text{ M}^{-1}$  as calculated by Job's plot and Benesi-Hildebrand plot. The chemosensor shows  $1.8 \times 10^{-8} \text{ M}$  detection limit, which is considerably lesser than that of the WHO admissible limit of [Cu<sup>2+</sup>] in drinking water. Possible interfering ions namely Ca<sup>2+</sup>, Mg<sup>2+</sup>, Fe<sup>2+</sup>, Co<sup>2+</sup>, Ni<sup>2+</sup>, Cd<sup>2+</sup>, Hg<sup>2+</sup>, Mn<sup>2+</sup>, Al<sup>3+</sup> and Cr<sup>3+</sup> do not show any appreciable interference in the colorimetric response of the probe towards Cu<sup>2+</sup>. Particularly, the colorimetric “ON-OFF-ON” responses are proved to be repeated over 5 times by the sequential inclusion of Cu<sup>2+</sup> and S<sup>2-</sup>. Sensitivity of the probe in real-time water and blood samples is found at par with results with AAS and ICP-OES techniques. Further, the reversibility of the probe and the easy fabrication of deployable strips for real-field naked eye detection of Cu<sup>2+</sup> suggest importance of synthesized probe.

© 2019 Elsevier B.V. All rights reserved.

### 1. Introduction

Among transition elements, copper is an essential and third most abundance among the required trace elements in the human body. It plays a critical role as a catalytic cofactor for a variety of metalloenzymes involved in transcriptional events [1] and other important fundamental physiological processes in various organisms [2]. However contamination of copper and its strong toxic effects on biological community are a threat, due to its wide use in domestic, agricultural and industrial practices [3]. Changes in the cellular balance of copper ion leads to serious disorders associated with neurodegenerative diseases like Wilson's disease [4], Menkes disease [5], Alzheimer's disease [6], Prion disease and familial amyotrophic lateral sclerosis [7]. The World Health Organization (WHO) has set the maximum granted limit of copper in drinking water at  $2 \text{ mgL}^{-1}$  ( $31 \text{ }\mu\text{M}$ ) [8]. Thus, event of authentic, easy and swift process for examining the copper quantity in environmental and biological samples is necessary. Numerous spectroscopic techniques [9] and electrochemical techniques [10] are implemented for Cu<sup>2+</sup> estimation

but they usually are time consuming, expensive and complicated. Optical spectroscopic techniques with fluorescent/non-fluorescent receptors have captivated researches attention with advantages like quick, sensitive and non-destructive study, low cost and prompt detection of metal ions by a simple enhancement in absorbance responses, the development and designing of colorimetric chemosensors for detection of biologically and environmentally important transition metal ions have received considerable importance [11]. Metal chalcogenide/quantum dots (QDs) have been reported as fluorescence based sensors/receptors with its excellent stability and photophysical properties [12]. Due to their tunable optical properties [12a,13], it has gained importance in numerous fields such as photovoltaics [14], bioimaging [15] and as sensors [16,17]. But unlike chemosensors it requires sophisticated instruments such as Spectrofluorophotometer and fluorescence microscope with skilled labor for sensing and can't be used as naked eye sensors based on color change. A number of receptors have been reported for the determination of Cu<sup>2+</sup> ions [18]. However, most of the recently delineated Cu<sup>2+</sup> sensors are quenching types [18e,19]. Characteristics like the interference of coexisting metal ions [18g,20], the convenient probability and the high response time still limit the practical application of Cu<sup>2+</sup> chemosensors. Number of chemosensors

\* Corresponding author.

E-mail address: [br.geetha@jainuniversity.ac.in](mailto:br.geetha@jainuniversity.ac.in) (R.G. Balakrishna).

has been developed for the consideration of more sensitive detection [21] and for their improvement with respect to water solubility. However reports on water-soluble chemosensors that can be employed in aqueous media do exist [18g,22]. Nevertheless, still there is a great scope and demand for novel and productive chemosensors for  $\text{Cu}^{2+}$ , particularly for those chemosensors that can function with high selectivity and sensitivity in aqueous media [23].

Colorimetric sensors for the detection of  $\text{Cu}^{2+}$  have some drawbacks like high response time [18g,24], poor sensitivity [1,18f,25], interference of other metal ions [26]. A bis-triazole-attached azobenzene chemosensor for selective sensing of  $\text{Cu}^{2+}$  was reported by Kannan et al. nonetheless the synthetic procedure of the same was a tiresome one [27], Sheng et al. detailed a test kit for colorimetric detection of  $\text{Cu}^{2+}$  with a detection limit of  $1.2\mu\text{M}$  [25]. Lu et al. reported a gold nanoparticle based sensor for selective and sensitive detection of  $\text{Cu}^{2+}$  with high response time but had  $\text{Co}^{2+}$  interference [28]. Despite their assertion of  $\text{Cu}^{2+}$  sensing in aqueous medium and still require  $\text{H}_2\text{O}/\text{DMSO}$  (60/40; v/v) solvent mixture. Gunnlaugsson et al. reported an azobenzene chemosensor for naked-eye detection of  $\text{Cu}^{2+}$  but  $\text{Cd}^{2+}$  and  $\text{Zn}^{2+}$  modulated the absorption spectrum of other metal ions at greater concentrations than that of  $\text{Cu}^{2+}$  [29]. Similarly, numerous of chemosensors described in the literature for detection of  $\text{Cu}^{2+}$  are on the basis of detection of multiple ion phenomenon [11b–d,30]. The chemosensors with multiple ion sensing are not demonstrated to be effective ones as there are possibilities of interference in the detection of targeted metal ion. Progress of economic, ion selective and naked eye detectable chemosensors are strongly in demand.

Rhodamine derivative based chemosensors, because of their excellent photo physical properties have attracted the attention of researchers. The spirolactam ring opening accords to a large molar extinction coefficient, absorption and emission at higher wavelengths, light stability etc. [11e]. Furthermore, the symmetry linking the nonfluorescent/noncolorimetric form and the highly fluorescent/colorimetric open-ring form anticipates a promising strategy to develop “turn-On” sensors. Hence, Rhodamine derivatives are extensively used as a colorimetric/fluorescent probe for the detection of various metal ions such as  $\text{Hg}^{2+}$  [11f],  $\text{Fe}^{3+}$  [11g],  $\text{Zn}^{2+}$  [31],  $\text{Cr}^{3+}$  [32],  $\text{Pb}^{2+}$  [33],  $\text{Au}^{3+}$  [34],  $\text{Al}^{3+}$  [35].

Exploring the chemosensors with above mentioned merits, herein we introduce ortho-Vanillin moiety to Rhodamine (probe **P**) which is highly selective and gives quick response to  $\text{Cu}^{2+}$  ion (Scheme 1). To the best of our knowledge, the synthesized probe is the first example of o-Vanillin based Rhodamine derivative as  $\text{Cu}^{2+}$  sensing probe. Our probe exhibits high selectivity and sensitivity compared to the recently developed  $\text{Cu}^{2+}$  sensors [36]. Use of immobilized probe strips for on-field naked eye detection, for real time industrial waste water analysis and for blood sample analysis shows its novelty and possible real time applications.

## 2. Experimental

### 2.1. Materials and methods

All the solvents used were of analytical grade and used without further purification, unless stated. Solvents were dried according to the standard procedures. Metals used are nitrates of  $\text{Hg}^{2+}$ ,  $\text{Cd}^{2+}$ ,  $\text{Co}^{2+}$ ,  $\text{Ni}^{2+}$ ,

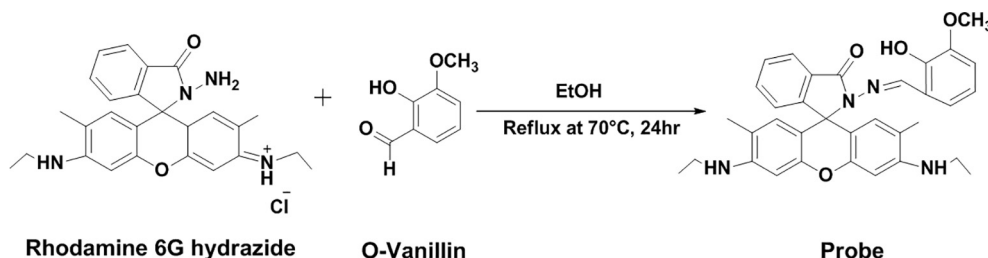
$\text{Mn}^{2+}$ ,  $\text{Zn}^{2+}$ ,  $\text{Mg}^{2+}$ ,  $\text{Ag}^{+}$ , and chloride salts of  $\text{Cr}^{3+}$ ,  $\text{Ca}^{2+}$ ,  $\text{Al}^{3+}$ ,  $\text{Fe}^{3+}$ ,  $\text{Pb}^{2+}$  and  $\text{Cu}^{2+}$  were commercially procured from Sigma-Aldrich Chemicals Co., and employed without any further purification. Throughout all the experiments double distilled water was used. All reactions were magnetically stirred and thin-layer chromatography (TLC) by Merck TLC Silica gel 60  $\text{F}_{254}$  coated plates were used to monitor the reaction. A JASCO-460 plus FT-IR spectrophotometer was utilized to carry out the FT-IR spectra of the samples as pressed KBr pellets. AAS measurements were carried out using Agilent 55B AA spectrometer. ICP-OES measurements were recorded Agilent 5100 VDV ICP-OES instrument. NMR spectroscopic measurements in  $\text{CDCl}_3$  were recorded with an Agilent spectrometer 400. The  $^1\text{H}$  NMR and  $^{13}\text{C}$  NMR chemical shift values are represented in ppm ( $\delta$ ) correlative to  $\text{CDCl}_3$ . Waters SynaptG2 LC-MS spectrometer was used to record the Mass spectra. Absorbance (UV-Vis) spectroscopic study was carried out with a Shimadzu UV-1800 spectrophotometer using quartz cuvette. X-ray Photoelectron Spectroscopy (XPS) analysis was performed with an Esca Pkxus Oxford XPS instrument.

### 2.2. Synthesis of probe

Rhodamine 6G Hydrazide was synthesized as per the reported procedure [18a], (see supporting information Figs. S1–S3). In 30 mL of absolute ethanol, Rhodamine 6G Hydrazide (0.48 g, 1 mmol) and ortho-Vanillin (0.28 g, 1.86 mmol) were dissolved, and the solution mixture was refluxed at  $70^\circ\text{C}$  for 24 h. The obtained compound was filtered and the residue was washed several times with absolute ethanol to remove any unreacted starting material. The purity of product was checked by spotting a product on chromatographed silica plate [60  $\text{F}_{254}$ ] with hexane/ethyl acetate (7:3, v/v) as eluent to get a light pink solid (probe **P**) in 85% yield. mp =  $256^\circ\text{C}$ .  $^1\text{H}$  NMR shows ( $\text{CDCl}_3$ , 400 MHz)  $\delta$  (ppm): 10.93 (1H, s, -CHO), 9.11 (1H, s,  $\text{CH}=\text{N}$ ), 7.96–7.98 (3H, Ar–H), 7.46–7.48 (3H, Ar–H), 7.24 (1H, Benzene-H), 7.05–7.05 (1H, d, Benzene-H), 6.78 (1H, t, Benzene-H), 6.70 (1H, d, Ben–H), 6.38 (2H, s, xanthene-H), 6.30 (2H, s, xanthene-H), 3.47–3.80 (2H,  $\text{NHCH}_2\text{CH}_3$ ), 3.20 (6H, q,  $\text{NHCH}_2\text{CH}_3$ ), 1.85 (6H, s, xanthene- $\text{CH}_3$ ), 1.30 (t, 6H,  $\text{NHCH}_2\text{CH}_3$ ).  $^{13}\text{C}$  NMR ( $\text{CDCl}_3$ )  $\delta$  (ppm): 14.7, 16.7, 38.2, 55.9, 66.2, 76.7, 77.0, 77.3, 96.9, 105.3, 113.2, 118.0, 118.4, 118.5, 123.2, 123.3, 123.9, 127.6, 128.3, 129.0, 133.5, 147.5, 148.1, 148.2, 151.5, 151.7, 152.7 and 164.5. ESI-MS, calculated for  $\text{C}_{34}\text{H}_{39}\text{O}_3\text{N}_4$   $m/z$  = 562.65, Found: 563.16 (see supporting information Figs. S4–S5).

### 2.3. Synthesis of $\text{Cu}^{2+}$ complex of probe

A 10 mL methanol solution of  $\text{CuCl}_2$  (1 mmol) was added slowly to a magnetically stirred solution of probe (1 mmol) in  $\text{CH}_3\text{CN}$ . The mixture was stirred for 10 min; a pink colored solution was obtained and left for slow evaporation, washed several times with distilled water and dried over vacuum. The corresponding IR and mass spectrum of the complex have been given in electronic supplementary information (Figs. S5 & S9). Spectroscopic characterization data for the complex: IR ( $\nu$ ,  $\text{cm}^{-1}$ ): 3320, 1607, 1498, 1444, 1372, 1302, 1182, 1126, 1081 and 1015. ESI-



Scheme 1. Synthesis scheme for the probe.

MS:  $m/z$ . Calculated for **P** +  $\text{Cu}^{2+}$  complex = 624.06 and found = 623.91.

#### 2.4. UV-Vis spectral studies

A stock solution of **P** ( $2.0 \times 10^{-5}$  M) was prepared in  $\text{CH}_3\text{CN}$ . Respective cations ( $1.0 \times 10^{-3}$  M) solutions were prepared in deionized water. For titration experiments, 2 mL ( $10 \mu\text{M}$ ) of probe solution was used in a quartz optical cell with an optical path length of 10 mm; Micropipette was used to add the metal ion stock and allowed to equilibrate the solution. After the addition of ions spectral data were recorded at 1 min. By adding appropriate amount of the anions/cations stock solution into 2 mL ( $10 \mu\text{M}$ ) probe solution, test samples were prepared for selectivity experiments. Reversibility study was done using  $1.0 \times 10^{-3}$  M solution of  $\text{S}^{2-}$  (aq.).

#### 2.5. Binding constants and stoichiometry calculation

The formation of the binding constant for respective complexes was evaluated using Benesi-Hildebrand (B-H) plot (Eq. (a)) [37].

$$1/(A - A_{\text{ini}}) = 1/K_a (A_{\text{max}} - A_{\text{ini}}) [\text{M}^{n+}] + 1/(A_{\text{max}} - A_{\text{ini}}) \quad (\text{a})$$

Here  $A_{\text{ini}}$ ,  $A_{\text{max}}$  and  $A$  represents the absorption potency of free probe, the maximal absorption intensity were pronounced at 523 nm at a certain concentration of the metal ion added. Binding stoichiometry for the formation of complex was also confirmed by Job's plot.

#### 2.6. Limit of detection

On the basis of the UV-Vis titration, limit of detection was calculated (Fig. 5b). The absorption spectrum of the probe was measured 25 times and the standard deviation of blank measurements was achieved. Plot of absorption intensity at 523 nm vs concentration of  $\text{Cu}^{2+}$  is used to calculate the slope. The limit of detection was deliberated with the following equation [38].

$$\text{DL} = (3 \times S_1)/S \quad (\text{b})$$

where DL (limit of detection),  $S_1$  is the standard deviation of a regression line and  $S$  is the slope.

#### 2.7. Fabrication of testing strips

Nitrocellulose strips were washed with distilled water followed by coating with poly vinyl alcohol (PVA) and dried. The dried strips were coated with probe and finally dried at room temperature. These strips were used for naked eye detection of  $\text{Cu}^{2+}$ .

#### 2.8. Computational studies

Gaussian 09 programs Becke's three parameterized Lee-Yang-Par (B3LYP) exchange functional with 6-31G\* basis sets were used to study the density functional theory (DFT) calculations for the optimization of the **P** and the **P** +  $\text{Cu}^{2+}$  complex.

#### 2.9. Detection of $\text{Cu}^{2+}$ in industry waste water and blood samples

Industrial waste water was collected from paper and plastic industry from Harohalli industrial area, Bangalore rural, Karnataka, India. Human whole blood samples were collected and samples were digested as per the established standard protocol [39]. Details of the certified reference material are attached in Fig. S14.

### 3. Results and discussions

#### 3.1. Designing of probe

The design of probe makes it a suitable candidate to function as an intramolecular charge transfer (ICT) probe. The xanthene part is expected to act as electron acceptor while the remaining part is expected to act as electron donor (Fig. 1). The effectiveness as an ICT probe was reproduced in terms of big perturbation in the absorption pattern as well as visual appearance (from colorless to pink) of the probe upon addition of  $\text{Cu}^{2+}$ . A strong intramolecular hydrogen bonding is quite likely between the -OH and imine =N which helps in blocking the possibility of anionic analytes interaction (Scheme 1).

#### 3.2. Visible detection of $\text{Cu}^{2+}$

Each metal ions like  $\text{Cr}^{2+}$ ,  $\text{Ag}^+$ ,  $\text{Cd}^{2+}$ ,  $\text{Fe}^{3+}$ ,  $\text{Al}^{3+}$ ,  $\text{Cu}^{2+}$ ,  $\text{Ca}^{2+}$ ,  $\text{Hg}^{2+}$ ,  $\text{Ni}^{2+}$ ,  $\text{Pb}^{2+}$  and  $\text{Zn}^{2+}$  were added separately to probe in  $10 \mu\text{M}$  solution. This displayed a recognizable color change from colorless to pink only for  $\text{Cu}^{2+}$  in  $\text{CH}_3\text{CN}$ , whereas other metal ions did not show any color change (Fig. 2). For this reason in case of  $\text{Cu}^{2+}$  easily observable color change with probe can be used for "naked eye" detection of  $\text{Cu}^{2+}$ . The emergence of the color change from colorless to pink was regarded to modulate the intramolecular charge transfer of probe upon effective coordination of  $\text{Cu}^{2+}$  through nitrogen atoms along with hydroxyl group of the probe.

#### 3.3. Effect of probe concentration, nature of the target analyte based on various anions and response time of the probe

The effect of probe concentration used for  $\text{Cu}^{2+}$  analysis was also investigated. Upon the addition of increasing amount of  $\text{Cu}^{2+}$  it looked like the concentration of probe was proportional to the absorbance maximum. But, within the dynamic range, the probe concentration did not play significant role in sensing of  $\text{Cu}^{2+}$ . In the following tests, the concentration of probe used was fixed to  $10 \mu\text{M}$ . According to the obtained results, the optimized condition selected for  $\text{Cu}^{2+}$  analysis was:  $10 \mu\text{M}$  in  $\text{CH}_3\text{CN}$  (Fig. S6a). The ability of the probe to detect  $\text{Cu}^{2+}$  present in various salt forms namely as  $\text{CuCl}_2$ ,  $\text{Cu}(\text{SO}_4)_4$  and  $\text{Cu}(\text{NO}_3)_2$  is investigated. The graph in Fig. S6b, shows more or less, a linear increase in the absorbance with concentration, for various analyte forms. The probe complex with copper, of  $\text{CuCl}_2$  has shown better sensitivity, compared to  $\text{Cu}(\text{NO}_3)_2$  and  $\text{CuSO}_4$ . The structure of anions could hence influence the sensitivity of the probe. The probe when complexed with  $\text{CuCl}_2$  shows a highly-linear curve indicating the accuracy of the

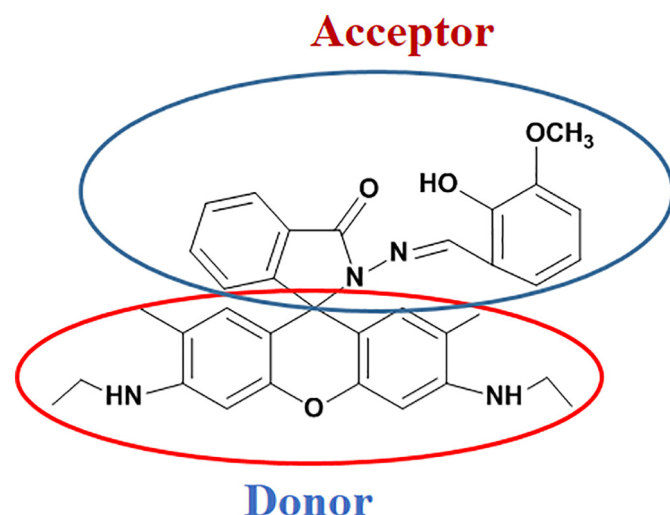


Fig. 1. Representation of donor and acceptor part of probe.

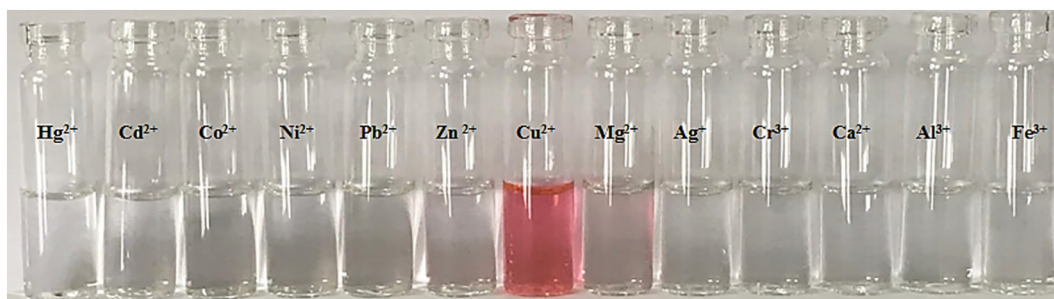


Fig. 2. Digital photograph of colorimetric changes of probe upon addition of various metal ions as their chloride salt.

results that would be obtained when  $\text{Cu}^{2+}$  is detected in  $\text{CuCl}_2$  salt forms. Favorable effect of anions on the probe complex follow the order  $\text{Cl}^- > \text{NO}_3^- > \text{SO}_4^{2-}$ , which is in accordance with distribution coefficient ( $\text{Log}_{10}\text{Kd}$ ) values. The response time of probe with  $\text{Cu}^{2+}$  was studied to examine the sensitivity of probe towards  $\text{Cu}^{2+}$ . As shown in Fig. S6c, the absorbance of probe at 527 nm rapidly increased with the addition of  $\text{Cu}^{2+}$  ( $10 \mu\text{M}$ ), reached maximum at 60 s and stabilized. These results indicate this probe is a sensitive chemosensor for the detection of  $\text{Cu}^{2+}$ .

### 3.4. Effect of pH

To investigate the influence of different acid-base concentration on the probe and to obtain a suitable pH in which probe can efficiently detect  $\text{Cu}^{2+}$ , the titration experiments were performed at various pH conditions ranging from 3 to 9. The probe by itself appeared pink at a pH below 3 i.e.; the probe lost its stability (was completely protonated) leading to spirolactam ring opening. The probe remains stable beyond pH 3. However, the sensitivity of the probe was highest at pH 6 which is attributed to opening of spirolactam ring as observed from Fig. S7. The formation of  $\text{Cu}(\text{OH})_2$  beyond pH 6 reduces the binding affinity and coordination tendency. Hence, pH 6 was considered as better operating pH.

### 3.5. Selectivity

Selectivity of probe towards  $\text{Cu}^{2+}$  among a wide range of biologically and environmentally important metal ions including  $\text{Cr}^{2+}$ ,  $\text{Ag}^+$ ,  $\text{Cd}^{2+}$ ,  $\text{Fe}^{3+}$ ,  $\text{Al}^{3+}$ ,  $\text{Cu}^{2+}$ ,  $\text{Ca}^{2+}$ ,  $\text{Hg}^{2+}$ ,  $\text{Ni}^{2+}$ ,  $\text{Pb}^{2+}$  and  $\text{Zn}^{2+}$  were investigated. Fig. 3 shows the absorption response of probe ( $10 \mu\text{M}$   $\text{CH}_3\text{CN}$ ) solution towards a series of the above mentioned metal ions. There was barely any change in the absorption spectra of the probe was observed but, under similar conditions, as we expected the probe was colorless and non-fluorescent due to the existence of nonconjugated spirolactam structural form of probe as shown in Scheme 1. The instant color change in presence of  $\text{Cu}^{2+}$  suggests that probe could serve as a “naked-eye” chemosensor for  $\text{Cu}^{2+}$  (Fig. 3 inset).

### 3.6. UV-Visible studies

With probe all spectroscopic measurements were performed in its  $10 \mu\text{M}$   $\text{CH}_3\text{CN}$  solution. The reaction of probe with  $\text{Cu}^{2+}$  was studied by UV-Vis titration. In the visible region the probe by itself showed almost nil absorption. The colorless probe solution turns pink and a new strong absorption band appears at 523 nm with increase in concentration of  $\text{Cu}^{2+}$  ions (Fig. 4). The “switch-On” behavior for the intense absorption peak at 523 nm suggests spirolactam ring opening in probe on  $\text{Cu}^{2+}$  coordination [40]. The isosbestic points at 255, 290 and 330 nm designates the formation of a single species between the probe and the  $\text{Cu}^{2+}$  (Fig. S8). The absorbance at 523 nm increases with  $\text{Cu}^{2+}$  concentration and saturates at  $\sim 250 \mu\text{molL}^{-1}$  of  $\text{Cu}^{2+}$ . There is no significant change in the absorbance when the concentration  $\text{Cu}^{2+}$  increases

from 250 to  $350 \mu\text{molL}^{-1}$ . Changes in the ultraviolet-visible (UV-Vis) absorption spectrum and the color change could be accompanied by the ligand-to metal charge transfer transition (Fig. 4). Absorbance of  $\text{Cu}^{2+}$  in  $\text{CH}_3\text{CN}$  was recorded (Fig. 4 inset) to rule out its effect on the absorbance of the probe.

The binding affinity of the  $\text{Cu}^{2+}$  towards the probe was evaluated from the spectrophotometric titration experiment using Benesi-Hildebrand plot and the binding constant ( $K_a$ ) is  $2.6 \times 10^4 \text{M}^{-1}$  and the correlation coefficient ( $R^2$ ) is 0.9829 (Fig. 5a). The detection limit of  $\text{Cu}^{2+}$  using probe is  $1.8 \times 10^{-8} \text{M}$  (Fig. 5b).

Job's plot results confirmed 1:1 binding stoichiometry for binding of  $\text{Cu}^{2+}$  and probe (Fig. 6a) which is further corroborated by mass spectra (Fig. S5b). Competitive binding of the probe to  $\text{Cu}^{2+}$  were determined in presence of other metal ions ( $500 \mu\text{molL}^{-1}$ ) like  $\text{Hg}^{2+}$ ,  $\text{Cd}^{2+}$ ,  $\text{Co}^{2+}$ ,  $\text{Ni}^{2+}$ ,  $\text{Mn}^{2+}$ ,  $\text{Zn}^{2+}$ ,  $\text{Mg}^{2+}$ ,  $\text{Ag}^+$ ,  $\text{Cr}^{3+}$ ,  $\text{Ca}^{2+}$ ,  $\text{Al}^{3+}$ ,  $\text{Fe}^{3+}$  and  $\text{Pb}^{2+}$  (Figs. 2, 6b). The UV-Vis spectral study confirms that probe selectively binds to  $\text{Cu}^{2+}$  in the presence of different metal ions. Competitive absorption response suggests that there is no significant interference by other metal ions and the probe selectively binds to the  $\text{Cu}^{2+}$ . This results further support that probe could serve as a sensitive naked eye chemosensor for  $\text{Cu}^{2+}$  detection.

### 3.7. Selective response of P + $\text{Cu}^{2+}$ media to various interfering anions

From the UV-Vis spectroscopic studies, we infer that probe selectively binds with  $\text{Cu}^{2+}$  to form P +  $\text{Cu}^{2+}$  complex with substantial change in its spectral behavior. One of the important features of the chemosensor is its elevated selectivity as well as the reversibility in

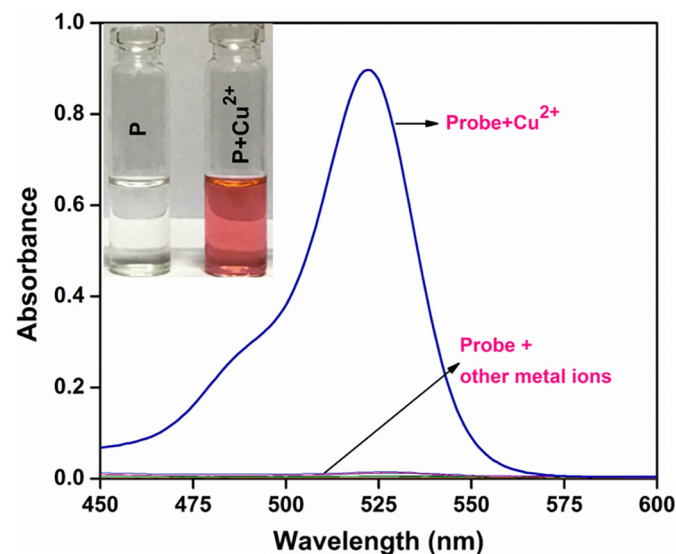


Fig. 3. Selectivity absorption changes of P upon addition various ions. Inset: L to R: digital photographs of P and P +  $\text{Cu}^{2+}$ .

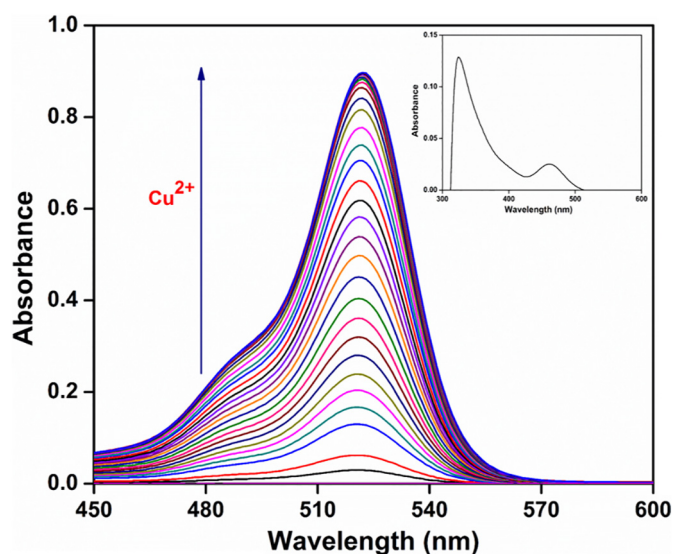


Fig. 4. UV-Vis titration spectra of probe with increasing  $\text{Cu}^{2+}$  ion concentration Inset: Absorbance of  $\text{Cu}^{2+}$  in  $\text{CH}_3\text{CN}$  (without the probe).

the complexation of any probe to be used as a chemical sensor for the determination of specific metal ions. Accordingly, we have measured the impact of different anions on the reversibility of  $\text{P} + \text{Cu}^{2+}$  complex to regenerate the probe. The probe could be revived by the addition of  $\text{S}^{2-}$  to the  $\text{P} + \text{Cu}^{2+}$  solution mixture (Figs. 7a, S12). Binding reversibility of  $\text{Cu}^{2+}$  to probe was also established in the presence of aq.  $\text{Na}_2\text{S}$  ( $500 \mu\text{mol L}^{-1}$ ) through UV-Vis spectral studies. Addition of  $\text{S}^{2-}$  to the  $\text{P} + \text{Cu}^{2+}$  complex leads to the reverse changes in the absorption spectra (Fig. S12). Additionally, for better understanding, we carried out UV-Vis titration for this complex. Upon addition of the  $\text{S}^{2-}$  (aq.) to the  $\text{P} + \text{Cu}^{2+}$  complex deep pink solution of  $\text{P} + \text{Cu}^{2+}$  complex at 523 nm absorption band disappears, as well as the solution become colorless (Fig. 7a, inset). The concentration of  $\text{S}^{2-} > 7.91 \times 10^{-7} \text{ M}$  alters the absorbance of  $\text{P} + \text{Cu}^{2+}$  which is calculated using LOD calculation (Fig. 7c). The dissociation constant of  $\text{Cu}^{2+}$  from  $\text{P} + \text{Cu}^{2+}$  complex upon addition of  $\text{S}^{2-}$  (which is calculated by change in absorbance of  $\text{P} + \text{Cu}^{2+}$  upon addition of  $\text{S}^{2-}$ ) is  $1.06 \times 10^5 \text{ M}^{-1}$  and a correlation coefficient ( $R^2$ ) is 0.9887 as evaluated from the spectrophotometric titration experiment using Benesi-Hildebrand plot (Fig. 7d). Again, upon addition of  $\text{Cu}^{2+}$  to the solution mixture having  $\text{S}^{2-}$ , restores the pink color of the solution and the absorption peak at 523 nm reappears. The IR spectra of  $\text{P} + \text{Cu}^{2+} + \text{S}^{2-}$  is in agreement with the spectra obtained for  $\text{P} + \text{Cu}^{2+}$  confirming the recyclability as shown in Fig. S13. Partial attachment of the  $\text{S}^{2-}$  ion to the  $\text{Cu}^{2+}$  ion leads to the formation of  $\text{CuS}$  and thus regenerates the cyclic spiriform of the probe [41]. This

reveals that signal process is reversible; hence, the chemosensor would be recyclable (Fig. S12).

### 3.8. Theoretical calculations

The probable binding fashion of the probe to  $\text{Cu}^{2+}$  was also explored with density functional theory (DFT) calculations. B3LYP method and general basis sets were used to optimize all geometries. Optimized structure of  $\text{P}$  and  $\text{P} + \text{Cu}^{2+}$  complex has shown in Fig. 7a and c respectively. HOMO of the probe suggests that a high electronic density resides on O, N atoms and thus these are the favorable binding site for the metal ions. As predicted,  $\text{Cu}^{2+}$  ion prefers to bind with O and N atoms and alpha and beta HOMO of  $\text{P} + \text{Cu}^{2+}$  complex is shown in Fig. 7d, e. Study revealed that the  $\text{P} + \text{Cu}^{2+}$  complex is  $-35.64 \text{ eV}$  more stable than separated reactants.

### 3.9. Mechanism of sensing

To understand the sensing behavior, we decided to analyze it by FTIR, LCMS, XPS and density functional theory (DFT) calculation. FTIR was used to examine the influence of  $\text{C}=\text{O}$  bond on binding  $\text{Cu}^{2+}$  ions. The peak at  $1690 \text{ cm}^{-1}$  is the characteristic stretching frequency for the  $\text{C}=\text{O}$  bond of the rhodamine unit. Upon binding to  $\text{Cu}^{2+}$  the peak at  $1690 \text{ cm}^{-1}$  disappears; suggest the breaking of  $\text{C}=\text{O}$  and the  $\text{Cu}^{2+}$  bonding with O-atom (Fig. S9). XPS characterization of probe and  $\text{P} + \text{Cu}^{2+}$  complex had been carried out to understand the fate of  $\text{Cu}^{2+}$  ion with probe (Fig. S10).  $\text{Cu}2\text{p}$  spectrum of the probe suggests the absence of copper ions (Fig. S10d). Peaks at 933.5 and 953.2 eV in  $\text{Cu}2\text{p}$  spectrum of  $\text{P} + \text{Cu}^{2+}$  complex corresponds to  $\text{Cu}2\text{p}_{3/2}$  and  $\text{Cu}2\text{p}_{1/2}$  respectively (Fig. S10). The peaks at 940.2, 944.5 eV corresponds to the strong satellite peak which confirms that Cu is in (II) oxidation state. The peak at 961.9 eV suggests the binding of  $\text{Cu}^{2+}$  with O-atom [42]. The N1 s peak becomes symmetrical in the  $\text{P} + \text{Cu}^{2+}$  complex (Fig. S10f) and shifts towards higher binding energy by 0.7 eV as compared to the bare probe (Fig. S10b) due to its interaction with  $\text{Cu}^{2+}$  ion. Shifting of N1s and O1s peak of  $\text{P} + \text{Cu}^{2+}$  complex as compared to probe towards higher binding energy suggests coordination of these atoms with  $\text{Cu}^{2+}$  ions. Additionally, to explore the colorimetric "On-Off" characteristics, the LCMS spectrum of the system [ $\text{P} + \text{Cu}^{2+} + \text{S}^{2-}$ ] was analyzed. In brief, after addition of  $\text{S}^{2-}$  solution to the  $\text{P} + \text{Cu}^{2+}$ , the resultant solution was centrifuged at 12,000 rpm for 30 min to remove the formed  $\text{CuS}$ . The supernatant was analyzed for LCMS. The peak at 563.27 confirm the formation of free probe upon addition of  $\text{S}^{2-}$  (mass of probe: 563.25 and mass of  $\text{P} + \text{Cu}^{2+}$ : 624.06) (Fig. S11). It is evident from  $\text{Cu}^{2+}$  binding studies that the binding leads to opening of the spirolactam ring of probe and that cause the color change. As demonstrated in Scheme 2, the addition of  $\text{Cu}^{2+}$  ion initiates colorimetric "On" response, generating a deep pink color.

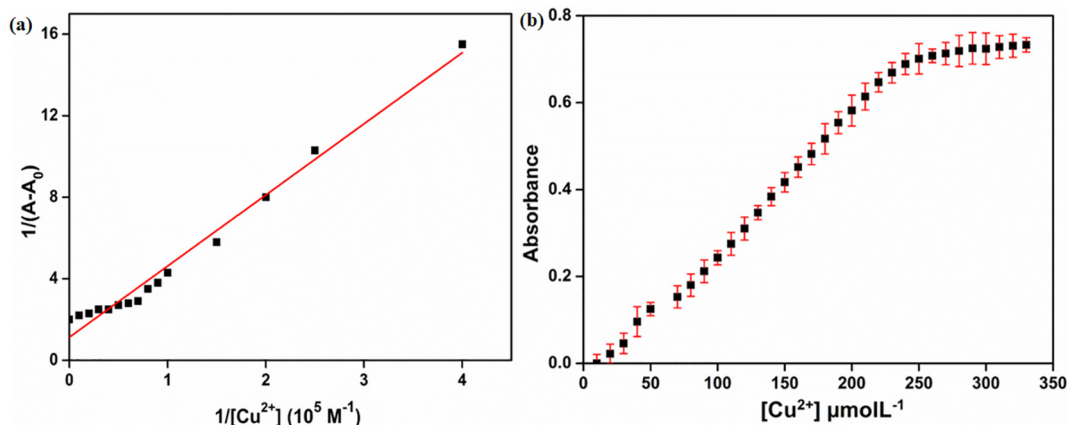


Fig. 5. (a) Benesi-Hildebrand plot. (b) Limit of detection calibration graph.

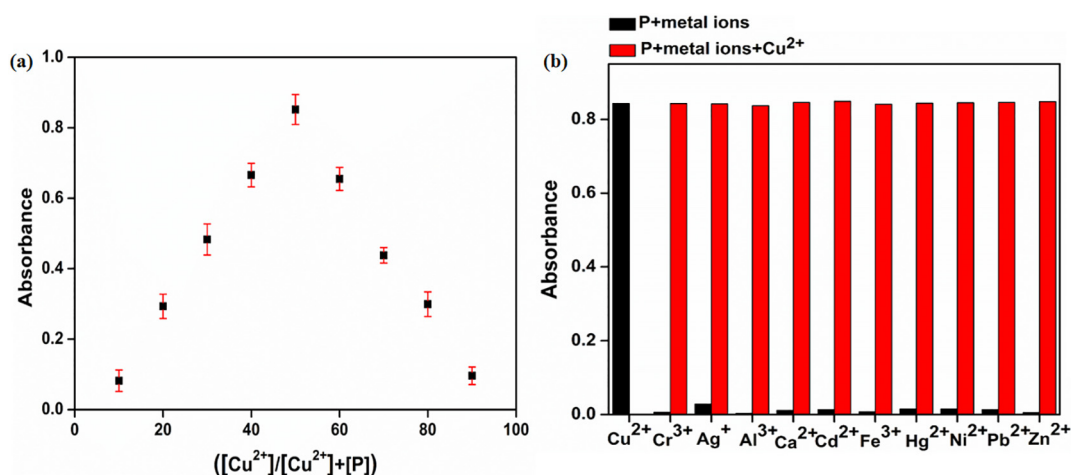


Fig. 6. (a) Job's plot (b) Effect of interfering cations to the absorption of the P + Cu<sup>2+</sup> complex.

Also, the added S<sup>2-</sup> can apprehend Cu<sup>2+</sup> ion, and induce a colorimetric change from deep pink to colorless (Fig. 8a, inset).

#### 4. Applications of probe

To assess the performance of a designed probe, real sample analysis is remarkable because of its viable impact from naturally occurring substances. The real-time implication of the probe was appraised through the determination of Cu<sup>2+</sup> ions in tap water, drinking water, industrial water and human blood samples. The water and blood samples were

also analyzed for Cu<sup>2+</sup> and validated by AAS and ICP-OES methods respectively. Samples were examined with their three replicates. The results acquired from this chemosensor are summarized in Tables 1 and 2. It can be seen from Tables 1 and 2, that the results obtained for water and human blood samples are in well accordance with AAS and ICP-OES. Therefore, the proposed colorimetric chemosensor has good practical feasibility in quantitative detection of copper in different environmental and biological samples. Therefore, the proposed colorimetric chemosensor has good practical feasibility in determination of copper in divergent samples.

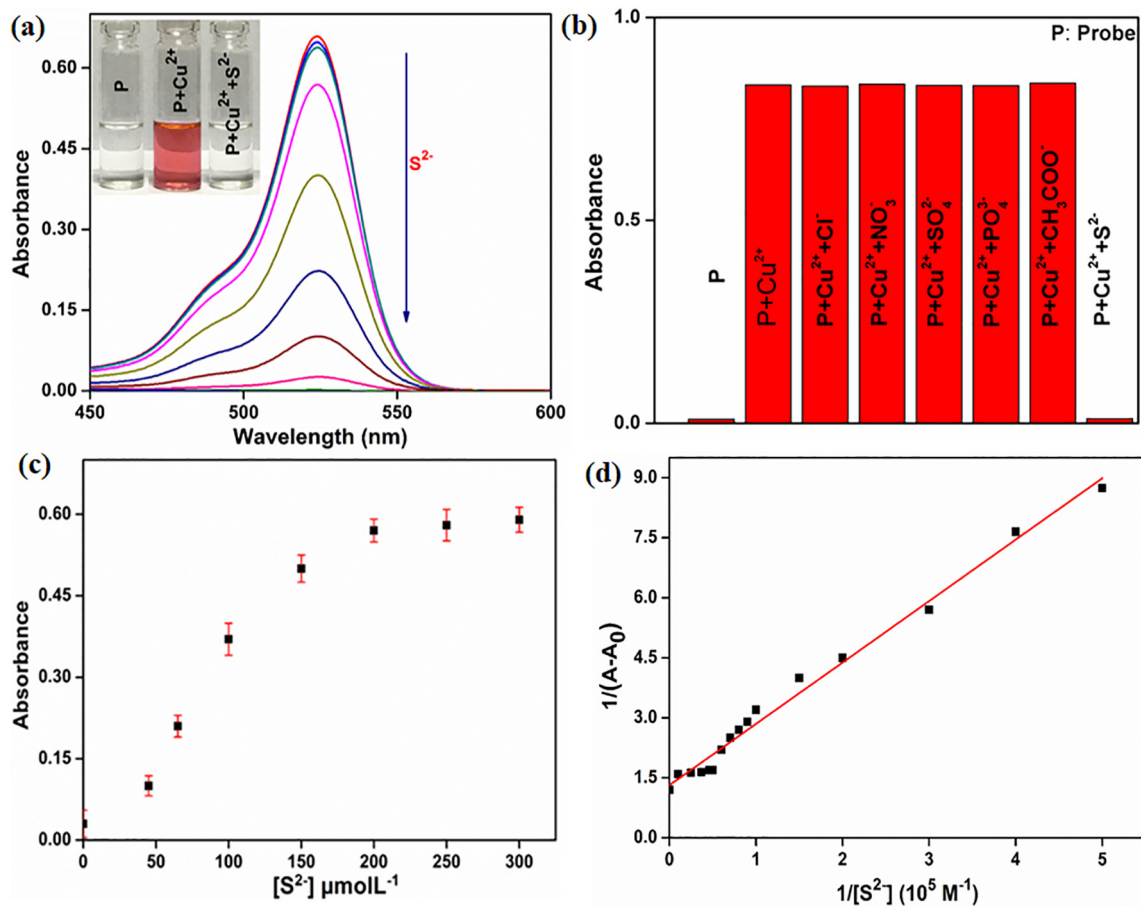
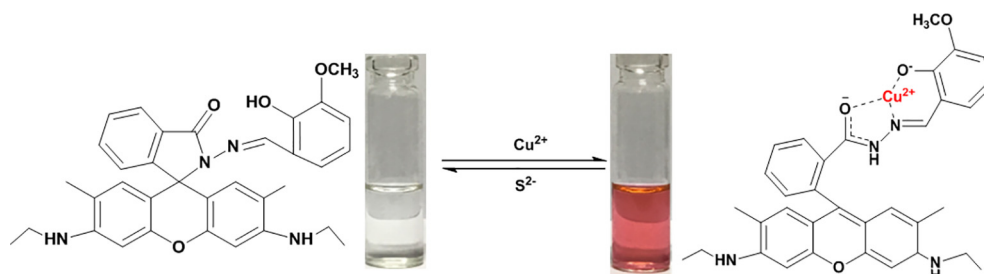
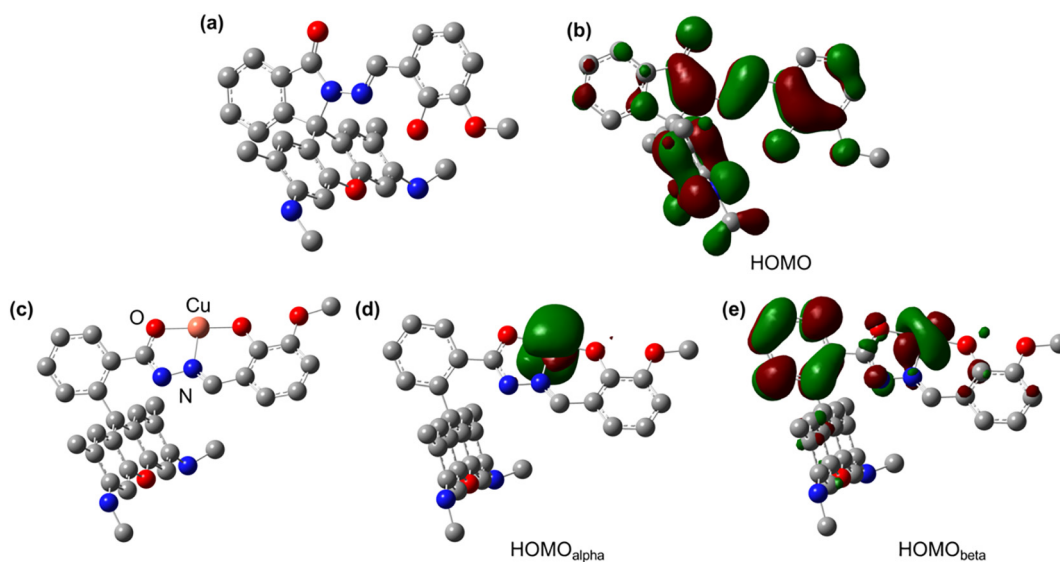


Fig. 7. (a) UV-Vis spectra showing reversibility of P + Cu<sup>2+</sup> complex upon addition of S<sup>2-</sup>. (b) Effect of anions to the absorption of the P + Cu<sup>2+</sup> complex. (c) Limit of detection calibration graph. (d) Benesi-Hildebrand plot.



**Scheme 2.** Proposed mechanism for the absorption changes in probe upon addition of  $\text{Cu}^{2+}$  and  $\text{S}^{2-}$ .



**Fig. 8.** (a) Optimized structure and (b) HOMO of P; (c) Optimized structure (d, e) alpha and beta HOMO of P +  $\text{Cu}^{2+}$  complex respectively.

**Table 1**  
Determination of  $\text{Cu}^{2+}$  in water samples.

Samples	AAS method		Present method	
	$\text{Cu}^{2+}$ found	RSD*(%)	$\text{Cu}^{2+}$ found	SE
Tap water	$7.74 \times 10^{-7}$ M	1.27	$7.91 \times 10^{-7}$ M	1.52
Drinking water	$7.56 \times 10^{-7}$ M	2.84	$7.21 \times 10^{-7}$ M	0.68
Industrial water	$1.50 \times 10^{-7}$ M	2.07	$1.31 \times 10^{-6}$ M	1.47

## 5. Test strips for quick detection of $\text{Cu}^{2+}$

Requirements for practical applications, portable testing strips were fabricated. The test strips were prepared by coating the nitrocellulose paper with PVA. The PVA coating neutralizes the charge on the surface of membrane partially and blocks the probe through hydrogen bonding hence making it viable for coating of the probe and then dried in air [43].

**Table 2**  
Determination of  $\text{Cu}^{2+}$  in blood samples.

Samples	ICP-OES method		Present method	
	$\text{Cu}^{2+}$ found	RSD*(%)	$\text{Cu}^{2+}$ found	SE
CBRM 1	$5.27 \times 10^{-7}$ M	5.24	$5.98 \times 10^{-7}$ M	1.94
CBRM 2	$5.27 \times 10^{-7}$ M	2.70	$5.86 \times 10^{-7}$ M	1.17
BS 1	$1.29 \times 10^{-6}$ M	0.03	$1.20 \times 10^{-6}$ M	0.88
BS 2	$1.40 \times 10^{-6}$ M	0.66	$1.31 \times 10^{-6}$ M	0.72

These test strips were directly used in the detection of  $\text{Cu}^{2+}$  solutions in various concentrations. The color change of the strips was observed only after treating them with  $\text{Cu}^{2+}$  solution (Fig. 9). The color change suggests the probe could be employed as portable tool for rapid and naked eye detection of  $\text{Cu}^{2+}$ .

Table 3 documented lately published research works on  $\text{Cu}^{2+}$  chemosensors. Our synthesized chemosensor has fairly high LOD, is highly sensitive and selective to  $\text{Cu}^{2+}$  ion.

## 6. Conclusion

We have reported an o-Vanillin functionalized Rhodamine 6G Hydrazide derivative as probe which exhibits high selectivity and sensitivity towards  $\text{Cu}^{2+}$  and over other important ions studied, viz.,  $\text{Hg}^{2+}$ ,  $\text{Cd}^{2+}$ .

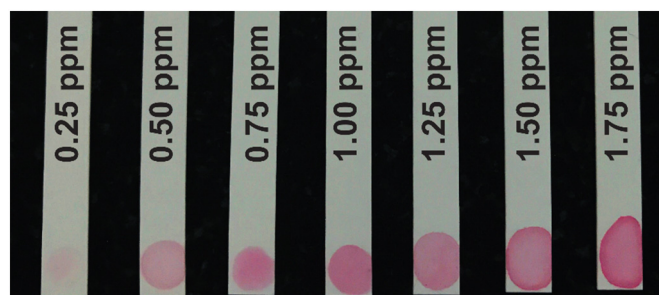


**Fig. 9.** Test strips for quick detection of  $\text{Cu}^{2+}$  (from L to R: concentration of  $\text{Cu}^{2+}$ ).

**Table 3**  
Comparative literature reports for Cu<sup>2+</sup> ion detection.

Sensing method	LOD for Cu <sup>2+</sup>	Reference
Colorimetric	2.0 × 10 <sup>-6</sup> M	[44]
Fluorometric	3.9 × 10 <sup>-6</sup> M	[45]
Colorimetric	2.9 × 10 <sup>-6</sup> M	[21b]
Fluorometric	2.3 × 10 <sup>-6</sup> M	[46]
Colorimetric	5.0 × 10 <sup>-6</sup> M	[47]
Colorimetric	2.9 × 10 <sup>-6</sup> M	[48]
Colorimetric	7.3 × 10 <sup>-10</sup> M	[22b]
Fluorometric	3.9 × 10 <sup>-6</sup> M	[45]
Colorimetric	1.2 × 10 <sup>-6</sup> M	[49]
Colorimetric	7.2 × 10 <sup>-7</sup> M	[11e]
Colorimetric	1.8 × 10 <sup>-8</sup> M	Present work

<sup>+</sup>, Co<sup>2+</sup>, Ni<sup>2+</sup>, Mn<sup>2+</sup>, Zn<sup>2+</sup>, Mg<sup>2+</sup>, Ag<sup>+</sup>, Cr<sup>3+</sup>, Ca<sup>2+</sup>, Al<sup>3+</sup>, Fe<sup>3+</sup>, and Pb<sup>2+</sup>, as manifested by titrations of individual as well as interfering metal ions. Interaction of the Cu<sup>2+</sup> with probe enhances the absorption intensity at 523 nm and causes a “turn-On” colorimetric response in the visible region and shows limit of detection to be 1.8 × 10<sup>-8</sup> M. The sensing mechanism of the probe has been evidenced by UV–Vis absorption, FTIR and LCMS spectroscopy. The binding mechanism elucidated from DFT studies revealed that the P + Cu<sup>2+</sup> complex is −35.64 eV more stable than individual reactants. The test strips made from probe could be employed as portable tool for rapid and naked eye detection of Cu<sup>2+</sup>. The reversible nature of the probe with high sensitivity may lead to the potential applications for the qualitative and quantitative detection of trace amounts of Cu<sup>2+</sup> in various chemical, environmental and biological samples.

### Declaration of Competing Interest

There are no conflicts to declare.

### Acknowledgment

The authors acknowledge BRNS, DAE, India for financial assistance (Project Sanction No: 37(2)14/06/2014-BRNS) and the Institute of Excellence, Vijnana Bhavana, University of Mysore, India for providing the Nuclear Magnetic Resonance (NMR) and Liquid Crystal Mass Spectrometry (LC-MS) facility also TUV India Private Limited, Bengaluru, India for providing ICP-OES instrumentation facility.

### Appendix A. Supplementary data

Supplementary data to this article can be found online at <https://doi.org/10.1016/j.saa.2019.117291>.

### References

- Xing Ma, a. Z. T., a Guohua Wei,\*a Dongbin Wei\*a and Yuguo Du\*a, Solvent controlled sugar–rhodamine fluorescence sensor for Cu<sup>2+</sup> detection†. *Analyst* 2012, 137 (2012), 1436.
- (a) Ling Mei, Y. X., Na Li, Aijun Tong \*, A new fluorescent probe of rhodamine B derivative for the detection of copper ion. *Talanta* 2007, 72 (200), 1717–1722; (b) D.W. Domaille, E.L. Que, C.J. Chang, Synthetic fluorescent sensors for studying the cell biology of metals, *Nat. Chem. Biol.* 4 (2008) 168.
- &, M. A. S. A. M. R. M. I.; & F. A. M. F. M. Z.-u.-R.; Bharwana 1, M. K. I. S. A., The effect of excess copper on growth and physiology of important food crops: a review. *Environ. Sci. Pollut. Res.* 2015, 22 (2015), 8148–8162.
- D. Huster, T.D. Purnat, J.L. Burkhead, M. Ralle, O. Fiehn, F. Stuckert, N.E. Olson, D. Teupser, S. Lutsenko, High copper selectively alters lipid metabolism and cell cycle machinery in the mouse model of Wilson disease, *J. Biol. Chem.* 282 (11) (2007) 8343–8355.
- (a) Daniel S. Yuan, R. S., Andrew DANcls, Teresa Dunnt, Troy Beelert, ; Klausnert, A. R. D., The Menkes/Wilson disease gene homologue in yeast provides copper to a ceruloplasmin-like oxidase required for iron uptake. *Proc. Nat L Acad Sc. USA* 1995, 92 (1995), 2632–2636.
- (b) Xie, X.; Mistlberger, G.; Bakker, E., Visible light induced photoacid generation within plasticized PVC membranes for copper (II) ion extraction. *Sensors and Actuators B: Chemical* 2014, 204, 807–810.
- a, M. S.; , C. M. b.; , U. O. c.; , M. A. S. d. 1; , W. M. K. a.; \*, Iron, zinc and copper in the Alzheimer's disease brain: a quantitative meta-analysis. Some insight on the influence of citation bias on scientific opinion. *Prog. Neurobiol.* 2011, 94 (2011), 296–306.
- A. Tiwari, L.J. Hayward, Familial amyotrophic lateral sclerosis mutants of copper/zinc superoxide dismutase are susceptible to disulfide reduction, *J. Biol. Chem.* 278 (8) (2003) 5984–5992.
- P.G. Georgopoulos, A. Roy, M.J. Yonone-Lioy, R.E. Opiekun, P.J. Lioy, Environmental copper: its dynamics and human exposure issues, *J Toxicol Environ Health B Crit Rev* 4 (4) (2001) 341–394.
- V. Iyengar, J. Woititez, Trace elements in human clinical specimens: evaluation of literature data to identify reference values, *Clin. Chem.* 34 (3) (1988) 474–481.
- (a) Xie, X.; Gutierrez, A.; Trofimov, V.; Szilagyi, I.; Soldati, T.; Bakker, E., Potassium sensitive optical nanosensors containing voltage sensitive dyes. *Chimia (Aarau)* 2015, 69 (4), 196–8.
- (b) J. Ding, T. Cherubini, D. Yuan, E. Bakker, Paper-supported thin-layer ion transfer voltammetry for ion detection, *Sensors Actuators B Chem.* 280 (2019) 69–76;
- (c) M. Cuartero, G. Crespo, In Situ Detection of Macronutrients and Chloride in Seawater by Submersible Electrochemical Sensors, vol. 90 (7), 2018 4702–4710;
- (d) J. Zhai, X. Xie, T. Cherubini, E. Bakker, Ionophore-based titrimetric detection of alkali metal ions in serum, *ACS Sensors* 2 (4) (2017) 606–612.
- (a) Paramjit Kaur a, Divya Sareena, Kamaljit Singhb, Selective colorimetric sensing of Cu<sup>2+</sup> using triazolyl monoazo derivative. *Talanta* 2011, 83 (2011), 1695–1700.
- (b) W. Yun, X. Du, J. Liao, G. Sang, L. Chen, N. Li, L. Yang, Three-way DNA junction based platform for ultra-sensitive fluorometric detection of multiple metal ions as exemplified for Cu(II), Mg(II) and Pb(II), *Mikrochim Acta* 185 (6) (2018) 306;
- (c) E. Feng, C. Fan, N. Wang, G. Liu, S. Pu, A highly selective diarylethene chemosensor for colorimetric detection of CN<sup>-</sup> and fluorescent relay-detection of Al<sup>3+</sup>/Cr<sup>3+</sup>, *Dyes Pigments* 151 (2018) 22–27;
- (d) Y.W. Choi, G.J. Park, Y.J. Na, H.Y. Jo, S.A. Lee, G.R. You, C. Kim, A single schiff base molecule for recognizing multiple metal ions: a fluorescence sensor for Zn(II) and Al(III) and colorimetric sensor for Fe(II) and Fe(III), *Sensors Actuators B Chem.* 194 (2014) 343–352;
- (e) Y. Li, X. Han, Y. Song, An azo-phenol derivative probe: colorimetric and “turn-on” fluorescent detection of copper(ii) ions and pH value in aqueous solution, *RSC Adv.* 7 (33) (2017) 20537–20541;
- (f) K. Ghosh, T. Sarkar, A. Samadder, A rhodamine appended tripodal receptor as a ratiometric probe for Hg<sup>2+</sup> ions, *Org. Biomol. Chem.* 10 (16) (2012) 3236–3243.
- (g) Zheng Yang, M. S., † Bing Yin, † Jihong Cui, † Yuze Zhang, † Wei Sun, † Jianli Li, † and Zhen Shi†, Three rhodamine-based “off–on” chemosensors with high selectivity and sensitivity for Fe<sup>3+</sup> imaging in living cells. *J. Org. Chem.* 2011.
- (a) H.R. Chandan, R. Geetha B, Study on precipitation efficiency of solvents in postpreparative treatment of nanocrystals, *J. Mater. Res.* 28 (21) (2013) 3003–3009.
- (b) R. C. H.; Venkataramana, M.; Kurkuri, M. D.; Balakrishna R G., Simple quantum dot bioprobe/label for sensitive detection of *Staphylococcus aureus* TNase. *Sensors Actuators B Chem.* 2016, 222, 1201–1208.
- H. Chandan, V. Saravanan, R.K. Pai, R.G. Balakrishna, Synergistic effect of binary ligands on nucleation and growth/size effect of nanocrystals: studies on reusability of the solvent, *J. Mater. Res.* 29 (14) (2014) 1556–1564.
- L.P. D'Souza, V. Amoli, H.R. Chandan, A.K. Sinha, R. Krishna Pai, G.R. Balakrishna, Atomic force microscopic study of nanoscale interaction between N719 dye and CdSe quantum dot in hybrid solar cells and their enhanced open circuit potential, *Sol. Energy* 116 (2015) 25–36.
- R.M. Renuka, J. Achuth, H.R. Chandan, M. Venkataramana, K. Kadirvelu, A fluorescent dual aptasensor for the rapid and sensitive onsite detection of *E. coli* O157:H7 and its validation in various food matrices, *New J. Chem.* 42 (13) (2018) 10807–10817.
- H. R. C.; Schiffman, J. D.; Balakrishna, R. G., Quantum dots as fluorescent probes: synthesis, surface chemistry, energy transfer mechanisms, and applications. *Sensors Actuators B Chem.* 2018, 258, 1191–1214.
- C. Hunsur Ravikumar, M. Ira Gowda, R.G. Balakrishna, An “OFF–ON” quantum dot-graphene oxide bioprobe for sensitive detection of micrococcal nuclease of *Staphylococcus aureus*, *Analyst* 144 (2019) 3999–4005.
- (a) Xiang, Y.; Li, Z.; Chen, X.; Tong, A., Highly sensitive and selective optical chemosensor for determination of Cu<sup>2+</sup> in aqueous solution. *Talanta* 2008, 74 (5), 1148–1153.
- (b) L. Chen, X. Tian, C. Yang, Y. Li, Z. Zhou, Y. Wang, F. Xiang, Highly selective and sensitive determination of copper ion based on a visual fluorescence method, *Sensors Actuators B Chem.* 240 (2017) 66–75;
- (c) Z. Xu, L. Zhang, R. Guo, T. Xiang, C. Wu, Z. Zheng, F. Yang, A highly sensitive and selective colorimetric and off-on fluorescent chemosensor for Cu<sup>2+</sup> based on rhodamine B derivative, *Sensors Actuators B Chem.* 156 (2) (2011) 546–552;
- (d) M.-J. Wu, H.-H. Hu, C.-Z. Siao, Y.-M. Liao, J.-H. Chen, M.-Y. Li, T.-Y. Lin, Y.-F. Chen, All organic label-like copper(II) ions fluorescent film sensors with high sensitivity and stretchability, *ACS Sensors* 3 (1) (2018) 99–105;
- (e) H.S. Jung, P.S. Kwon, J.W. Lee, J.I. Kim, C.S. Hong, J.W. Kim, S. Yan, J.Y. Lee, J.H. Lee, T. Joo, J.S. Kim, Coumarin-derived Cu<sup>2+</sup>-selective fluorescence sensor: synthesis, mechanisms, and applications in living cells, *J. Am. Chem. Soc.* 131 (5) (2009) 2008–2012;
- (f) L. Tang, F. Li, M. Liu, R. Nandhakumar, Single sensor for two metal ions: colorimetric recognition of Cu<sup>2+</sup> and fluorescent recognition of Hg<sup>2+</sup>, *Spectrochim. Acta A Mol. Biomol. Spectrosc.* 78 (3) (2011) 1168–1172;



- (g) S. Paul, A. Manna, S. Goswami, A differentially selective molecular probe for detection of trivalent ions ( $\text{Al}^{3+}$ ,  $\text{Cr}^{3+}$  and  $\text{Fe}^{3+}$ ) upon single excitation in mixed aqueous medium, *Dalton Trans.* 44 (26) (2015) 11805–11810.
- [19] (a) Minglei Zhao, X.-F. Y., Shenfeng He, Liping Wang, A rhodamine-based chromogenic and fluorescent chemosensor for copper ion in aqueous media. *Sensors and Actuators B* 2009, 135 (2009), 625–631.  
(b) Z. Xu, X. Qian, J. Cui, Colorimetric and ratiometric fluorescent chemosensor with a large red-shift in emission:  $\text{Cu}(\text{II})$ -only sensing by deprotonation of secondary amines as receptor conjugated to naphthalimide fluorophore, *Org. Lett.* 7 (14) (2005) 3029–3032.
- [20] (a) Shyamaprosad Goswami, A. M., Krishnendu Aich, and Sima Paul, A simple rhodamine-based naked-eye and fluorescence "OffOn" sensor for  $\text{Cu}(\text{II})$  in aqueous solution, *Chemical Letters* 2012, 41 (2012), 1600–1602.  
(b) C.M.G. van den Berg, Chemical speciation of iron in seawater by cathodic stripping voltammetry with dihydroxynaphthalene, *Anal. Chem.* 78 (1) (2006) 156–163.
- [21] (a) Gupta, V. K.; Singh, A. K.; Kumawat, L. K.; Mergu, N., An easily accessible switch-on optical chemosensor for the detection of noxious metal ions  $\text{Ni}(\text{II})$ ,  $\text{Zn}(\text{II})$ ,  $\text{Fe}(\text{III})$  and  $\text{UO}_2(\text{II})$ , *Sensors Actuators B Chem.* 2016, 222, 468–482.  
(b) G.J. Park, G.R. You, Y.W. Choi, C. Kim, A naked-eye chemosensor for simultaneous detection of iron and copper ions and its copper complex for colorimetric/fluorescent sensing of cyanide, *Sensors Actuators B Chem.* 229 (2016) 257–271.
- [22] (a) Li, Z.; Zhang, Y.; Xia, H.; Mu, Y.; Liu, X., A robust and luminescent covalent organic framework as a highly sensitive and selective sensor for the detection of  $\text{Cu}^{2+}$  ions. *Chem. Commun.* 2016, 52 (39), 6613–6616.  
(b) R. Chandra, A. Ghorai, G.K. Patra, A simple benzildihydrazone derived colorimetric and fluorescent "on-off-on" sensor for sequential detection of copper(II) and cyanide ions in aqueous solution, *Sensors Actuators B Chem.* 255 (2018) 701–711.
- [23] (a) Lin Wang, X. G., Qijing Bing, Guang Wang, Lin Wang, Xue Gong, Qijing Bing, Guang Wang, *Microchemical Journal* 2018, 142 (2018).  
(b) H. Shao, Y. Ding, X. Hong, Y. Liu, Ultra-facile and rapid colorimetric detection of  $\text{Cu}(2+)$  with branched polyethylenimine in 100% aqueous solution, *Analyst* 143 (2) (2018) 409–414.
- [24] (a) Kaur, P.; Sareen, D.; Singh, K., Selective colorimetric sensing of  $\text{Cu}^{2+}$  using triazolyl monoazo derivative. *Talanta* 2011, 83 (5), 1695–700.  
(b) J.Y. Noh, G.J. Park, Y.J. Na, H.Y. Jo, S.A. Lee, C. Kim, A colorimetric "naked-eye"  $\text{Cu}(\text{II})$  chemosensor and pH indicator in 100% aqueous solution, *Dalton Trans.* 43 (15) (2014) 5652–5656.
- [25] R. Sheng, P. Wang, Y. Gao, Y. Wu, W. Liu, J. Ma, H. Li, S. Wu, Colorimetric test kit for  $\text{Cu}^{2+}$  detection, *Org. Lett.* 10 (21) (2008) 5015–5018.
- [26] R.-L. Liu, H.-Y. Lu, M. Li, S.-Z. Hu, C.-F. Chen, Simple, efficient and selective colorimetric sensors for naked eye detection of  $\text{Hg}^{2+}$ ,  $\text{Cu}^{2+}$  and  $\text{Fe}^{3+}$ , *RSC Adv.* 2 (10) (2012) 4415–4420.
- [27] E. Hrishikesan, C. Saravanan, P. Kannan, Bis-triazole-appended azobenzene chromophore for selective sensing of copper(II) ion, *Ind. Eng. Chem. Res.* 50 (13) (2011) 8225–8229.
- [28] C.-H. Lu, Y.-W. Wang, S.-L. Ye, G.-N. Chen, H.-H. Yang, Ultrasensitive detection of  $\text{Cu}^{2+}$  with the naked eye and application in immunoassays, *Npg Asia Materials* 4 (2012) e10.
- [29] T. Gunnlaugsson, J.P. Leonard, N.S. Murray, Highly selective colorimetric naked-eye  $\text{Cu}(\text{II})$  detection using an azobenzene chemosensor, *Org. Lett.* 6 (10) (2004) 1557–1560.
- [30] (a) Kaur, P.; Kaur, S.; Singh, K.; Sharma, P. R.; Kaur, T., Indole-based chemosensor for  $\text{Hg}^{2+}$  and  $\text{Cu}^{2+}$  ions: applications in molecular switches and live cell imaging, *Dalton Trans.* 2011, 40 (41), 10818–10821.  
(b) Ming Xua, C. Y., \*, Fangjun Huo b,\*\*, Yongbin Zhang b, Jianbin Chao b, A highly sensitive "ON-OFF-ON" fluorescent probe with three binding sites to sense copper ion and its application for cell imaging. *Sensors Actuators B* 2014, 204 (18–23).
- [31] P. Du, S.J. Lippard, A highly selective turn-on colorimetric, red fluorescent sensor for detecting mobile zinc in living cells, *Inorg. Chem.* 49 (23) (2010) 10753–10755.
- [32] S. Saha, P. Mahato, U.R. G. E. Suresh, A. Chakrabarty, M. Baidya, S.K. Ghosh, A. Das, Recognition of  $\text{Hg}^{2+}$  and  $\text{Cr}^{3+}$  in physiological conditions by a rhodamine derivative and its application as a reagent for cell-imaging studies, *Inorg. Chem.* 51 (1) (2012) 336–345.
- [33] J.Y. Kwon, Y.J. Jang, Y.J. Lee, K.M. Kim, M.S. Seo, W. Nam, J. Yoon, A highly selective fluorescent chemosensor for  $\text{Pb}^{2+}$ , *J. Am. Chem. Soc.* 127 (28) (2005) 10107–10111.
- [34] J. Young Choi, G.-H. Kim, Z. Guo, H. Yeon Lee, K.M.K. Swamy, J. Pai, S. Shin, I. Shin, J. Yoon, Highly selective ratiometric fluorescent probe for  $\text{Au}^{3+}$  and its application to bioimaging, *Biosens. Bioelectron.* 49 (2013) 438–441.
- [35] A. Sahana, A. Banerjee, S. Lohar, B. Sarkar, S.K. Mukhopadhyay, D. Das, Rhodamine-based fluorescent probe for  $\text{Al}^{3+}$  through time-dependent PET-CHEF-FRET processes and its cell staining application, *Inorg. Chem.* 52 (7) (2013) 3627–3633.
- [36] X.G. Lin Wang, Qijing Bing, Guang Wang, A new oxadiazole-based dual-mode chemosensor: colorimetric detection of  $\text{Co}^{2+}$  and fluorometric detection of  $\text{Cu}^{2+}$  with high selectivity and sensitivity, *Microchemical Journal* 142 (2018) (2018) 279–287.
- [37] X. Bao, Q. Cao, X. Wu, H. Shu, B. Zhou, Y. Geng, J. Zhu, Design and synthesis of a new selective fluorescent chemical sensor for  $\text{Cu}^{2+}$  based on a pyrrole moiety and a fluorescein conjugate, *Tetrahedron Lett.* 57 (8) (2016) 942–948.
- [38] Y. Gao, H. Liu, Q. Liu, W. Wang, A novel colorimetric and OFF-ON fluorescent chemosensor based on fluorescein derivative for the detection of  $\text{Fe}^{3+}$  in aqueous solution and living cells, *Tetrahedron Lett.* 57 (17) (2016) 1852–1855.
- [39] (a) Mahalingam, T. R.; Vijayalakshmi, S.; Prabhu, R. K.; Thiruvengadasami, A.; Mathews, C. K.; Shanmugasundaram, K. R., Studies on some trace and minor elements in blood. A survey of the Kalpakkam (India) population. Part I: standardization of analytical methods using ICP-MS and AAS. *Biol. Trace Elem. Res.* 1997, 57 (3), 191–206.  
(b) B. Ivanenko N, A. Ganeev, N. Solovyev, L. Moskvin, Determination of Trace Elements in Biological Fluids, vol. 66, 2011 784–799.
- [40] Z.L. Yu Xiang, Xiaotong Chen, Aijun Tong \*, Highly sensitive and selective optical chemosensor for determination of  $\text{Cu}^{2+}$  in aqueous solution, *Talanta* 74 (2008) (2007) 1148–1153.
- [41] Zhihong Xua, Like Zhanga, Rui Guoa,c, Tiancheng Xianga, Changzeng Wua, Zhi Zheng b, F. Y. b., c,\*, A highly sensitive and selective colorimetric and off-on fluorescent chemosensor for  $\text{Cu}^{2+}$  based on rhodamine B derivative, *Sensors Actuators B* 2011 (156) (2011) 546–552.
- [42] Miaomiao Chen, a. Y. D., a Yan Gao, a Xixi Zhu, a Peng Wang, a Zhiqiang Shi\*<sup>b</sup>; Liu Q. \*<sup>a</sup>, a., N,N0-di-carboxy methyl perylene diimide (PDI)functionalized  $\text{CuO}$  nanocomposites with enhanced peroxidase like activity and their application in visual biosensing of  $\text{H}_2\text{O}_2$  and glucose†. *RSC Adv.* 2017, 7 (2017), 25220–25228.
- [43] H.T. Uyeda, I.L. Medintz, J.K. Jaiswal, S.M. Simon, H. Mattoussi, Synthesis of compact multidentate ligands to prepare stable hydrophilic quantum dot fluorophores, *J. Am. Chem. Soc.* 127 (11) (2005) 3870–3878.
- [44] J.Z. Yang Hu, Yuan-Zheng Lv, Xiao-Huan Huang, Sheng Li, A.T.a.L.J. Hayward†, A new rhodamine-based colorimetric chemosensor for naked-eye detection of  $\text{Cu}^{2+}$  in aqueous solution, *Spectrochim. Acta A Mol. Biomol. Spectrosc.* 157 (2015) 164–169.
- [45] A new oxadiazole-based dual-mode chemosensor: colorimetric detection of  $\text{Co}^{2+}$  and fluorometric detection of  $\text{Cu}^{2+}$  with high selectivity and sensitivity, *Microchem. J.* 2018 (142) (2018) 279–287.
- [46] M.A.K. Soumen Ghosh, Aniruddha Ganguly Abdulla, M.A.A. Al Masum, Nikhil Guchhait, Binding mode dependent signaling for the detection of  $\text{Cu}^{2+}$ : an experimental and theoretical approach with practical applications, *Spectrochim. Acta A Mol. Biomol. Spectrosc.* 190 (2017) 471–477.
- [47] Tonmoy Ghoshi<sup>1</sup>, 3 & Apeksha Vyas<sup>4</sup> & Khushbu Bhayani<sup>1</sup> & Sandhya Mishra<sup>1,2</sup>, C-phycoerythrin as a colorimetric and fluorometric probe for the sensitive, selective and quantitative detection of  $\text{Cu}^{2+}$  in aqueous samples. *J. Fluoresc.* 2018.
- [48] Gyeong Jin Park, G. R. Y., Ye Won Choi, Cheal Kim\*: Department, A naked-eye chemosensor for simultaneous detection of iron and copper ions and its copper complex for colorimetric/fluorescent sensing of cyanide. *Sensors Actuators B* 2016.
- [49] Hong Shao, Y. D., Xia Hong\* and Yichun Liu, Ultra-facile and rapid colorimetric detection of  $\text{Cu}^{2+}$  with branched polyethylenimine in 100% aqueous solution. *Analyst* 2017, 00 (2017), 1–5.